

# Ratchetlike Properties of In Vitro Microtubule Translocation by a *Chlamydomonas* Inner-Arm Dynein Species *c* in the Presence of Flow

Kenji Kikushima and Ritsu Kamiya\*

Department of Biological Sciences, Graduate School of Science, University of Tokyo, Tokyo, Japan

**ABSTRACT** To investigate the force generation properties of *Chlamydomonas* axonemal inner-arm dyneins in response to external force, we analyzed microtubule gliding on dynein-coated surfaces under shear flow. When inner-arm dynein *c* was used, microtubule translocation in the downstream direction accelerated with increasing flow speed in a manner that depended on the dynein density and ATP concentration. In contrast, the microtubule translocation velocity in the upstream direction was unaffected by the flow speed. The number of microtubules on the glass surface was almost constant with and without flow, suggesting that gliding acceleration was not simply caused by weakened dynein-microtubule binding. With other inner-arm dynein species, the microtubule gliding velocity was unaffected by the flow regardless of the flow direction or nucleotide concentration. The flow-generated force acting on a single dynein was estimated to be as small as  $\sim 0.03$  pN/dynein. These results indicate that dynein *c* possesses a ratchetlike property that allows acceleration only in one direction by a very small external force. This property should be important for slow- and fast-moving dyneins to function simultaneously within the axoneme.

## INTRODUCTION

The beating of cilia and flagella depends on the controlled sliding between adjacent outer-doublet microtubules, which is driven by dynein molecules that constitute the outer and inner dynein arms. Studies using *Chlamydomonas* have shown that the outer dynein arm comprises a single assembly containing three discrete heavy chains, the mechanochemical enzymes that produce force. In contrast, the inner-arm dynein comprises multiple species, each containing one or two heavy chains (1,2). Altogether, the axoneme has as many as 14 dynein heavy chains (3,4).

The motility of mutant axonemes lacking a particular set of dyneins, as well as the microtubule-translocating properties of each dynein species in vitro, indicates that various dyneins significantly differ in their motile properties (5–9). For example, microtubule translocation velocities on glass surfaces coated with *Chlamydomonas* inner-arm dyneins vary between 2 and 11  $\mu\text{m/s}$  depending on the dynein species (8). Mutant flagella lacking any one species of dynein display lower motility than wild-type, and those lacking certain combinations of dyneins are paralyzed. These observations indicate that each dynein species contributes to efficient axonemal beating, and that the presence of certain combinations of dyneins is essential for beating.

The question that arises from such results is how dyneins that move at different speeds cooperate in the axoneme to produce regular beating. If the axoneme exhibited a simple sliding movement, the simultaneous presence of slow and fast motors would be inefficient, since the slow motors

would act as a drag on the fast motors. However, the axoneme is a complex molecular machine in which microtubule sliding takes place at various speeds depending on the bending wave phase. At a certain time and position within the axoneme, a pair of doublet microtubules undergoes an active shearing motion in one direction driven by the dyneins arranged on one of the doublets. At another time point, the same pair undergoes a passive shearing motion in the opposite direction after active sliding between another outer doublet pair. Thus, each dynein molecule in the axoneme is always subjected to forces of varying magnitude and direction produced by other dynein molecules.

We speculated that axonemal dyneins might have special properties that enable diverse dyneins to function in the axoneme without sacrificing efficiency. For example, force production by some dyneins might sensitively vary depending on the curvature of the axoneme or the sliding velocity of the outer doublets. To explore such hypothetical special properties, we examined the behavior of *Chlamydomonas* inner-arm dyneins in the presence of a force produced by shear flow. We found that an inner-arm dynein species, dynein *c*, displayed a ratchetlike response to the external force, such that the microtubule translocation velocity was influenced only by external flow in one direction. We suggest that this ratchetlike property is one of the mechanisms that allow dyneins with different intrinsic speeds to function simultaneously.

## MATERIALS AND METHODS

### Preparation of inner-arm dyneins

Dyneins were prepared from the *Chlamydomonas reinhardtii* mutant *odal* lacking outer-arm dyneins, as described elsewhere (8). In brief, isolated

Submitted March 29, 2009, and accepted for publication July 8, 2009.

\*Correspondence: kamiyar@biol.s.u-tokyo.ac.jp

Kenji Kikushima's present address is Department of Molecular Neurobiology, Tokyo Metropolitan Institute for Neuroscience, Tokyo, Japan.

Editor: Hideo Higuchi.

© 2009 by the Biophysical Society  
0006-3495/09/09/1657/6 \$2.00

doi: 10.1016/j.bpj.2009.07.010

flagella were demembrated with Nonidet P40 and extracted with 0.6 M KCl. The crude dynein extract was fractionated into seven inner-arm dynein species (a–g) by HPLC on a MonoQ column (Fig. 1 A).

## In vitro motility assay

In vitro motility assays were performed essentially as reported previously (9) (Fig. 1 B). Each dynein species (0.06 mg/mL) in HMDE solution (30 mM Hepes, 5 mM MgSO<sub>4</sub>, 1 mM DTT, 1 mM EGTA, pH 7.4) was introduced into a flow chamber (internal size: 18 × 5 × 0.08 mm) made of a glass slide, coverslip, and pair of spacers. The chamber containing dynein was incubated for 3 min, followed by introduction of HMDE containing 2 mg/mL bovine serum albumin. After a microtubule solution (8 μM) in HMDE was introduced into the chamber, microtubule translocation was initiated by perfusing the chamber with reactivation solution (HMDE containing 10 μM taxol with appropriate concentrations of ATP and 0.1 mM ADP). ADP was included because it has a stimulatory effect on the motile activity of inner-arm dyneins (10,11). When the activation solution contained ≥25 mM K-acetate or when the dynein density was low (≤0.01 mg/mL), the microtubules were easily detached from the dynein-coated surface. Under these conditions, we added 2 μM microtubules to the reactivation solution to supplement microtubules that tended to be lost during perfusion.

Shear flow was applied to the microtubules by perfusing the chamber with buffer solution using a peristaltic pump. The flow speeds in the chamber are not uniform, since microtubules on the surface experience lower flow speeds than those of the flow in the central region between the two surfaces. An estimation of the flow speed distribution is given below.

The flow direction was determined from the movement of small bubbles flowing in the plane of the gliding microtubules. Microtubule polarity was determined from the direction of movement in the absence of flow; the advancing front was defined as the plus end, since all inner-arm dyneins are minus-end-directed motors (8). The microtubule gliding velocity did not change after repeated application of flow in either direction, indicating that the flow did not significantly deteriorate the condition of dyneins on the glass surface during a series of experiments. Microtubule translocation was observed with a darkfield microscope equipped with a ×50 objective (NA: 0.90) and an SIT camera (C2400-08; Hamamatsu Photonics, Hamamatsu City, Japan). The spatial resolution of the total system is ~0.35 μm, and the time resolution is ~33 ms. The microtubule gliding velocity was measured by tracing the end position of each microtubule at appropriate intervals (~1 s). For each data point (except those shown in Fig. 4), ~25 different microtubule images were used to obtain the average and standard deviation (SD; shown as an error bar). Under our observation conditions, microtubules did not attach to glass surfaces without adsorbed dynein. Therefore, what we measured in this study was the velocity of the microtubules attached on the glass surface through their interactions with dynein, and not that of the free-floating microtubules. Images were video-recorded and analyzed with an in-house-developed software program.

## Estimate of the force acting on a single gliding microtubule

We assume that the medium flows parallel to the chamber wall and behaves as a Poiseuille flow with a viscosity identical to that of water ( $\eta = 8.9 \times 10^{-4} \text{ Pa} \cdot \text{s}$ ). The local flow speed of medium  $u(y)$  at distance  $y$  from the glass slide follows the equation  $d^2u/dy^2 = -a/\eta$ , where  $a$  is a constant (12). At the surface, the flow speed is zero:  $u(0) = 0$  and  $u(h = 80 \mu\text{m}) = 0$ , where  $h$  is the distance between the glass slide and the coverslip. Therefore, we get  $u(y) = ya/2\eta(h - y)$ . The flow rate  $Q$  is given by  $Q = \int u(y) dy dz$  ( $y = 0$  to  $h$ ) ( $z = 0$  to  $w$ , the width of the chamber (5 mm)) =  $awh^3/12\eta$ . Thus,  $u(y) = (6Q/wh^3) y(h - y)$ . At a standard flow rate of 103 μL/min, the local flow speed of medium  $y$  μm above the glass slide is  $u(y)$  (μm/s) =  $4.0 \times y(80 - y)$ . Since the approximate size of a dynein molecule is 40 nm and the radius of microtubule is 12.5 nm, the average flow speed around the microtubules is  $u(52.5 \text{ nm}) = 17 \mu\text{m/s}$ . The fluid speed at the surface changes greatly depending on the distance from the surface (for example, if  $y$  increases from 40 to 60 nm,  $u$  changes from 13 to 19 μm/s), and the effective medium velocity around a gliding microtubule varies depending on the direction of the microtubule gliding with relative to the flow direction. This flow speed (subtracted by the microtubule gliding velocity) is proportional to the shear force acting on a unit length of microtubule. The drag coefficient per unit length of microtubule parallel to the flow is estimated to be  $c = 2\pi\eta / \ln(2y/r) = 2.6 \times 10^{-3} \text{ (N} \cdot \text{s/m}^2)$ , where  $r$  is the radius of a microtubule (12.5 nm) (13,14). Therefore, the external force acting on a stopped microtubule is  $cu = 2.6 \times 10^{-3} \text{ (N} \cdot \text{s/m}^2) \times 17 \mu\text{m/s} = 0.04 \text{ pN}/\mu\text{m}$ . The force acting on microtubules gliding in the direction of flow must be significantly lower than this value because they experience lower relative flow velocity.

## RESULTS

The motile properties of various axonemal dynein species have been studied by assaying microtubule translocation on dynein-coated glass surfaces (8,15,16). To study the force generation properties of inner-arm dyneins in response to external force, we performed in vitro motility assays while applying shear flow. For most of the inner-arm dynein species examined, including dynein *c*, application of flow (flow rate: 103 μL/min) for 3 min changed the microtubule gliding direction such that >90% of the microtubules came to move in approximately the direction of flow (Fig. 1 C). For inner-arm dyneins *d* and *g*, each microtubule tended to glide at a shallow right-handed angle to the flow, and not exactly parallel to the flow (9). However, in all cases, most microtubules tended to move downstream. Similar

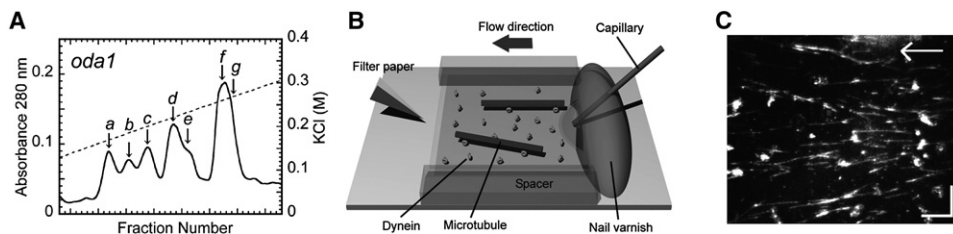


FIGURE 1 Experimental procedures. (A) Separation of *Chlamydomonas* inner-arm dyneins. Crude dynein extract from *oda1* (a mutant lacking outer-arm dynein) was fractionated into seven inner-arm dynein species (dyneins a–g) by HPLC with a MonoQ column. (This figure is from Kikushima and Kamiya (9).) Solid line: Absorbance at 280 nm. Dotted line: KCl concentration.

(B) Flow chamber for the in vitro motility assay. The internal size was 18 × 5 × 0.08 mm. Flow was applied by perfusing the chamber with a buffer solution using a peristaltic pump and a piece of filter paper placed on the opposite side of the chamber. In some experiments, flow direction was reversed by operating the pump backward. In this case, a large drop of medium was placed by the open side of the chamber so as to supply the medium into the chamber. (C) Darkfield images of microtubules on the dynein *c*-coated glass surface at 3 min after application of shear flow. Arrow indicates the direction of flow. Scale bars: 10 μm. Flow rate of the medium: 103 μL/min. ATP: 0.5 mM. ADP: 0.1 mM.

downstream microtubule gliding has been observed with kinesin (17); however, in that case, the polarity of the microtubules must be opposite. The microtubule gliding direction was most likely changed by the flow because the shear force bends the advancing front of each microtubule to the downstream direction, and the lagging portion of each microtubule advances following the front portion (9,17). Because the change in microtubule orientation occurred rather slowly after flow application, we were able to measure the velocity of microtubules gliding either upstream or downstream by quickly reversing the flow direction. Flow speeds for the microtubules gliding upstream and downstream were designated with minus and plus signs, respectively.

Microtubule translocation driven by dynein *c* displayed a peculiar dependence on the shear flow (Fig. 2). At low ATP concentrations ( $\sim 0.1$  mM), the velocity did not change upon application of flow in either direction. However, at  $\geq 0.5$  mM ATP, the velocities of microtubules moving downstream increased with increasing flow speed. In contrast, the velocities of microtubules moving upstream

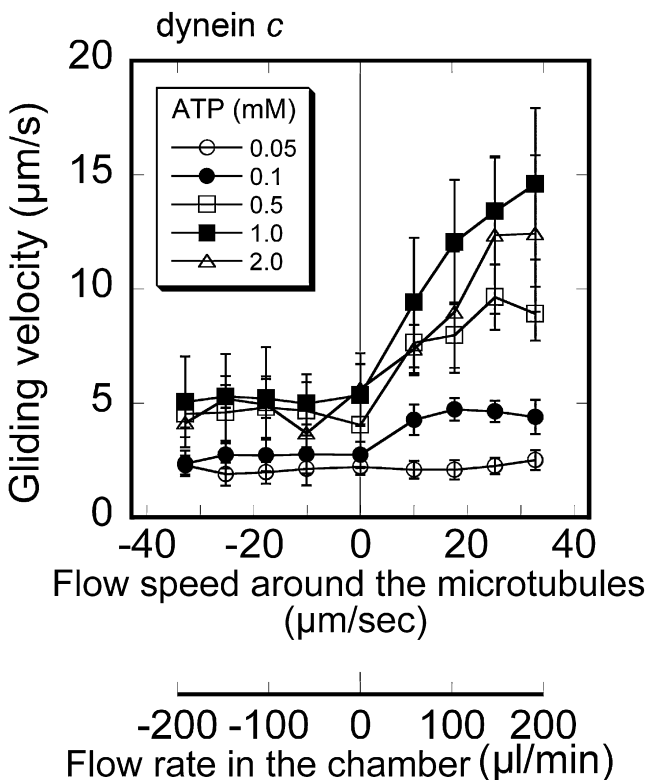


FIGURE 2 Velocities of microtubules gliding on glass surfaces covered with dynein *c* in the presence of flowing medium. Gliding velocities of microtubules moving backward to the flow were measured by quickly reversing the flow direction. The flow speed for microtubules moving against the flow is designated by a minus sign. The flow speed (*upper scale*) around the microtubules was estimated from the flow rate of the peristaltic pump (*bottom scale*) and the equations given in the *Materials and Methods*. Different symbols denote experiments at different ATP concentrations. ATP: 0.05–2.0 mM. ADP: 0.1 mM. Each data point with an error bar represents the average and SD in  $\sim 25$  samples.

were unaffected by the flow speed. These results indicate that, at a higher ATP concentration, the response of dynein *c* to the external force is asymmetric with respect to the force direction. Dynein *c* apparently has a ratchetlike property that allows it to be moved by an external force directed only in the forward direction. In contrast to dynein *c*, the other inner-arm dyneins did not display a marked flow-dependent change in microtubule gliding speed, regardless of the flow direction or nucleotide concentration (dyneins *d* and *g*; Fig. 3). Therefore, the mechanical response to flow may differ among dynein species.

To examine whether the binding between dynein *c* and microtubules was affected by the flow in a direction-sensitive manner, we counted the number of microtubules gliding downstream or upstream after the application, removal, or reversal of flow. After the removal of flow, the number of microtubules on the glass surface remained almost unchanged (Fig. 4 A), although the direction of microtubule translocation became gradually randomized (9). Upon application of flow, only a negligible fraction of microtubules detached from dynein *c*-coated glass surfaces (Fig. 4 B). When the flow direction was reversed, the microtubule gliding direction gradually changed to the flow direction (Fig. 4 C), but the total number of microtubules attached to the surface did not show a marked change. These observations indicate that flow in either direction does not promote microtubule dissociation from dynein *c*-coated glass surfaces. Therefore, the flow-induced increase in microtubule gliding speed is apparently not simply caused by reducing the binding force between the dynein and microtubules.

The flow-dependent microtubule gliding by dynein *c* was found to be sensitive to the ionic strength of the medium. The microtubule gliding velocities, advancing in either flow direction, decreased when the K-acetate concentration of the medium was  $\leq 50$  mM, regardless of the flow rate (Fig. 5 A). However, at higher concentrations ( $\geq 75$  mM), the microtubules easily detached from the glass surface (data not shown), and gliding in both directions was greatly affected by flow. This change in flow sensitivity is likely due to a change in the affinity between the dynein and microtubules.

The flow dependence of the microtubule gliding velocity was also dependent on the dynein concentration (Fig. 5 B). When the concentration was  $< 0.01$  mg/mL, microtubules easily detached from the glass surface, and the gliding velocity was greatly increased by flow in the forward direction.

## DISCUSSION

In this study, we examined the effect of media flow on in vitro microtubule translocation by *Chlamydomonas* inner-arm dyneins. Dynein *c* displayed an asymmetrical response to external force with respect to the force direction: the microtubule gliding velocity accelerated in the presence

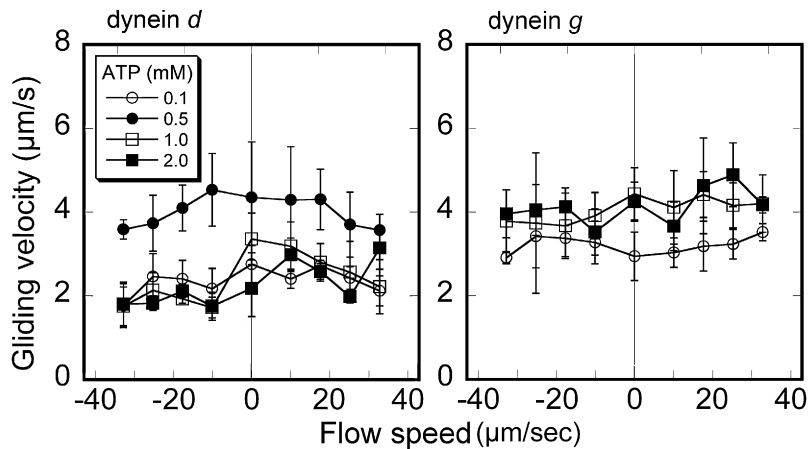


FIGURE 3 Velocities of microtubules gliding on glass surfaces covered with dyneins *d* and *g* in the presence of shear flow. ATP: 0.1–2.0 mM. ADP: 0.1 mM.

of forward flow, but did not decelerate in the presence of backward flow. To our knowledge, such a peculiar response to external force has not been reported for any other motor proteins examined *in vitro*. At the same time, we did not observe similar asymmetric behavior in dyneins *d* and *g*. This may indicate a fundamental difference between these dyneins and dynein *c*. Alternatively, dyneins *d* and *g* may also display an asymmetric response to a greater force or under different conditions. Whether these and other axonemal dyneins respond to stronger forces in a symmetric or asymmetric manner remains an important question. Dynein *c* has been shown to be a unique motor in that it displays a processive movement even though it is single-headed and has a low duty ratio (18). The relationship between the ratchetlike properties and the processivity of dynein *c* also remains to be elucidated.

The magnitude of the flow-generated force in our experiment must be very small. At the most frequently used setting (estimated flow speed around the microtubules: 17  $\mu\text{m/s}$ ), the force acting on a single microtubule oriented parallel to the flow was estimated to be  $\sim 0.04$  pN/ $\mu\text{m}$  (see [Materials and](#)

[Methods](#)). Assuming that 10% of all dynein molecules in the chamber were bound to the glass surface in a functionally active manner (18), the dynein concentration on the surface was 500 dyneins/ $\mu\text{m}^2$ . Further assuming that each dynein can interact with a microtubule within a 20 nm radius (19),  $\sim 10$  dynein molecules are expected to interact with microtubules per micrometer. The number of dynein molecules firmly bound to a microtubule per micrometer was calculated to be 1.4 ( $10 \times 0.14$ , the reported duty ratio of dynein *c* (18)). Therefore, the force acting on a single dynein is  $0.04$  pN/ $1.4 = 0.03$  pN. Although this estimate is very rough and the true value could differ by as much as an order of magnitude, it is clear that dynein *c* responds to a very small forward force, much smaller than the maximal force produced by dynein (1–2 pN) (18).

In this context, we must consider that the force produced under almost load-free conditions is much smaller than the stall force, since the force produced by dynein must be equal to the frictional force acting on the gliding microtubule. Because the microtubule gliding velocity displayed by dynein *c* in the absence of flow is  $\sim 5$   $\mu\text{m/s}$  and the flow rate near

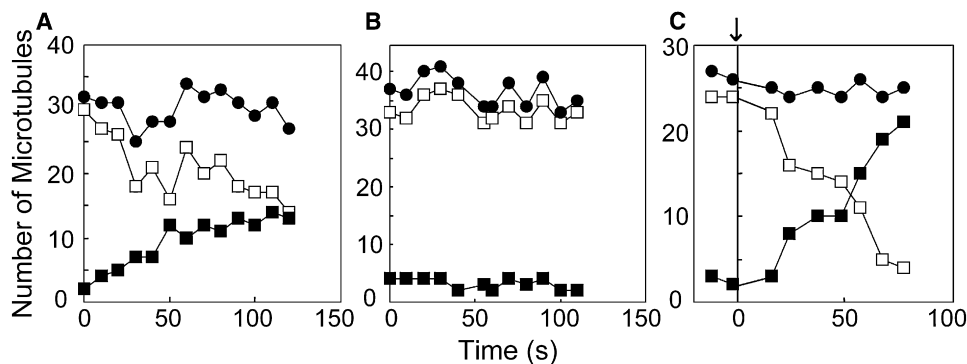


FIGURE 4 Change in the number of microtubules gliding on a dynein *c*-coated glass surface after application or removal of medium flow. The number of microtubules in a  $40 \mu\text{m} \times 40 \mu\text{m}$  area was counted. (A and B) Change in the number of microtubules on the glass slide after cessation (A) or application (B) of flow at time 0. (C) Change in the number of microtubules when the flow direction was reversed at time 0. Open squares denote the number of microtubules gliding in the forward direction to the flow, solid squares denote those gliding in the opposite direction, and solid circles denote the total number of microtubules present on the glass surface. The arrow indicates the time when the flow direction was reversed. Flow rate of the medium: 103  $\mu\text{L/min}$ . ATP: 0.5 mM. ADP: 0.1 mM.

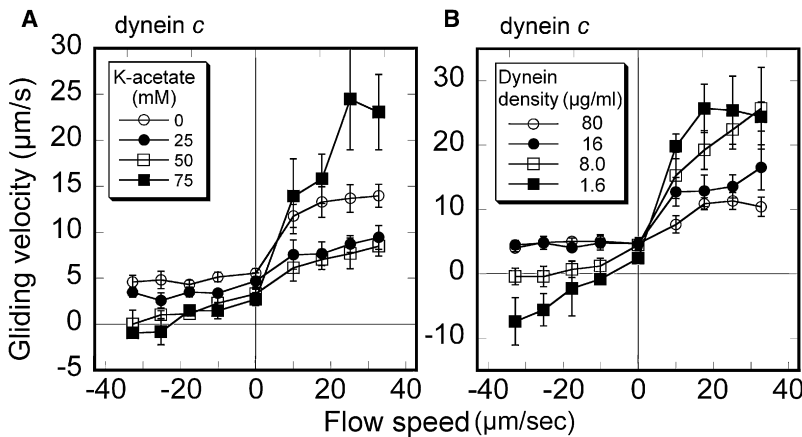


FIGURE 5 Effect of ionic strength (A) and dynein concentration (B) on the gliding velocities of microtubules under flow. Experimental conditions were the same as those in Fig. 3 except that the K-acetate concentration was varied between 0 and 75 mM in A, and the dynein concentration was varied between 1.6 and 80  $\mu\text{g}/\text{mL}$  in B. Microtubule polarity was determined by measuring the gliding direction in the absence of flow. ATP: 1.0 mM. ADP: 0.1 mM.

gliding microtubules was estimated to be  $\sim 17 \mu\text{m}/\text{s}$  (see [Materials and Methods](#)), dynein *c* is accelerated by a forward-directing force with a magnitude similar to the force it produces without load. This force dependence of the gliding velocity is clearly different from that observed in an actin-myosin system, where a much greater force ( $\sim 10\%$  of the maximal force) is required to produce any effects on the *in vitro* translocation of myosin-coated beads. Of interest, in that case, application of force in the forward direction decelerates, rather than accelerates, the bead movement (20).

The molecular mechanism of the asymmetric response of dynein *c* to such small external forces remains to be elucidated. An asymmetric response could occur if a step(s) in the mechanochemical cycle of the dynein-microtubule interaction is sensitive to external forces in an asymmetric manner, such as due to the anisotropic nature of protein-protein interactions. Alternatively, an asymmetry could be produced by the presence of an auxiliary, asymmetric interaction independent of primary motor interaction (21). Asymmetric responses to external forces of opposing directions have recently been proposed for kinesin and myosin V, homodimeric motor proteins that move processively by alternating their two motor domains (heads) in a hand-over-hand fashion. In these motors, simultaneous binding of the two heads to a microtubule or actin filament causes internal strains that act on each one of the two heads in opposite directions. In the currently prevailing models, the oppositely directed strains are thought to cause different effects on the two heads, such as the acceleration/deceleration of ATP binding or ADP release, ensuring the alternating movements of the two heads (for review see Gennerich and Vale (22)). Although the force postulated in such a model for myosin and kinesin is much greater (on the order of pico-Newtons), such a direction-dependent mechanosensitivity may well be functioning in the ratchetlike behavior of dynein *c*.

Since microtubule gliding by dynein *c* is accelerated by a very small forward force, we can surmise that dynein *c* does not impose a significant drag on a microtubule moving faster than the sliding speed that this dynein can produce. Previous analyses of microtubule sliding velocities in mutant

axonemes have suggested that outer-arm dyneins are much faster motors than inner-arm dyneins (23). However, it has been unclear why the sliding velocity in mutant axonemes lacking several species of inner-arm dyneins is almost the same as that in wild-type axonemes, and it is hard to understand why slow-moving inner-arm dyneins in the wild-type axoneme do not retard the sliding movement caused by outer-arm dyneins. This study provides a clue to answer this question: some inner-arm dyneins may well have an intrinsic property that allows them to follow the faster microtubule movement produced by outer-arm dyneins without significantly retarding it.

This study was supported by a grant from the Japan Society for Promotion of Science, and by the Global Centers of Excellence program "Integrative Life Science Based on the Study of Biosignaling Mechanisms" of the Ministry of Education, Culture, Sports, Science, and Technology of Japan.

## REFERENCES

- Kamiya, R. 2002. Functional diversity of axonemal dyneins as studied in *Chlamydomonas* mutants. *Int. Rev. Cytol.* 219:115–155.
- King, S. M., and R. Kamiya. 2009. Axonemal dyneins: assembly, structure and force generation. *In The Chlamydomonas Sourcebook*, Vol. III. G. B. Witman, editor. Elsevier Press, Amsterdam, The Netherlands. 129–206.
- Porter, M. E., J. A. Knot, S. H. Myster, and S. J. Farlow. 1996. The dynein gene family in *Chlamydomonas reinhardtii*. *Genetics*. 144:569–585.
- Yagi, T., K. Uematsu, Z. Liu, and R. Kamiya. 2009. Identification of novel dyneins that localize exclusively to the proximal portion of *Chlamydomonas* flagella. *J. Cell Sci.* 122:1306–1314.
- Brokaw, C. J., and R. Kamiya. 1987. Bending patterns of *Chlamydomonas* flagella: IV. Mutants with defects in inner and outer dynein arms indicate differences in dynein arm function. *Cell Motil. Cytoskeleton*. 8:68–75.
- Sale, W. S., and L. A. Fox. 1988. Isolated  $\beta$ -heavy chain subunit of dynein translocates microtubules *in vitro*. *J. Cell Biol.* 107:1793–1797.
- Moss, A. G., J. L. Gatti, and G. B. Witman. 1992. The motile  $\beta/\text{IC1}$  subunit of sea urchin sperm outer arm dynein does not form a rigor bond. *J. Cell Biol.* 118:1177–1188.
- Kagami, O., and R. Kamiya. 1992. Translocation and rotation of microtubules caused by multiple species of *Chlamydomonas* inner-arm dynein. *J. Cell Sci.* 103:653–664.

9. Kikushima, K., and R. Kamiya. 2008. Clockwise translocation of microtubules by flagellar inner-arm dyneins in vitro. *Biophys. J.* 94:4014–4019.
10. Yagi, T. 2000. ADP-dependent microtubule translocation by flagellar inner-arm dyneins. *Cell Struct. Funct.* 25:263–267.
11. Kikushima, K., T. Yagi, and R. Kamiya. 2004. Slow ADP-dependent acceleration of microtubule translocation produced by an axonemal dynein. *FEBS Lett.* 563:119–122.
12. Kambe, T. 2007. *Elementary Fluid Mechanics*. World Scientific, Hackensack, NJ.
13. Hunt, A. J., F. Gittes, and J. Howard. 1994. The force exerted by a single kinesin molecule against a viscous load. *Biophys. J.* 67:766–781.
14. Howard, J. 2001. *Mechanics of Motor Proteins and the Cytoskeleton*. Sinauer Associates, Sunderland, MA.
15. Paschal, B. M., S. M. King, A. G. Moss, C. A. Collins, R. B. Vallee, et al. 1987. Isolated flagellar outer arm dynein translocates brain microtubules in vitro. *Nature*. 330:672–674.
16. Vale, R. D., and Y. Y. Toyoshima. 1988. Rotation and translocation of microtubules in vitro induced by dyneins from *Tetrahymena* cilia. *Cell*. 52:459–469.
17. Stracke, R., K. J. Böhm, J. Burgold, H. J. Schacht, and E. Unger. 2000. Physical and technical parameters determining the functioning of a kinesin-based cell-free motor system. *Nanotechnology*. 11:52–56.
18. Sakakibara, H., H. Kojima, Y. Sakai, E. Katayama, and K. Oiwa. 1999. Inner arm dynein *c* of *Chlamydomonas* flagella is a single-headed processive motor. *Nature*. 400:586–590.
19. Duke, T., T. E. Holy, and S. Leibler. 1995. “Gliding assays” for motor proteins: a theoretical analysis. *Phys. Rev. Lett.* 74:330–333.
20. Oiwa, K., S. Chaen, E. Kamitsubo, T. Shimmen, and H. Sugi. 1990. Steady-state force-velocity relation in the ATP-dependent sliding movement of myosin-coated beads on actin cables in vitro studied with a centrifuge microscope. *Proc. Natl. Acad. Sci. USA*. 87:7893–7897.
21. Brokaw, C. J. 2001. Protein-protein ratchets: stochastic simulation and application to processive enzymes. *Biophys. J.* 81:1333–1344.
22. Gennerich, A., and R. D. Vale. 2009. Walking the walk: how kinesin and dynein coordinate their steps. *Curr. Opin. Cell Biol.* 21:59–67.
23. Kurimoto, E., and R. Kamiya. 1991. Microtubule sliding in flagellar axonemes of *Chlamydomonas* mutants missing inner- or outer arm dynein: velocity measurements on new types of mutants by an improved method. *Cell Motil. Cytoskeleton*. 19:275–281.